

Muon Catalyzed Fusion, Present and Future

Atsuo Iiyoshi^{1, a)}, Yasushi Kino^{2, b)}, Motoyasu Sato^{1, c)}, Yoshiharu Tanahashi¹,
Norimasa Yamamoto¹, Shin Nakatani¹, Takuma Yamashita³, Michael Tendler^{1, 4},
and Osamu Motojima^{1, a)}

¹Chubu University, 1200 Matsumoto, Kasugai, Aichi, Japan

²Tohoku University, 6-3, Aramaki Aza-Aoba, Aoba-ku, Sendai, Miyagi, Japan

³RIKEN, 2-1 Hirosawa, Wako, Saitama, Japan

⁴KTH, Royal Institute of Technology, Stockholm, Sweden

^{a)}Corresponding authors: iiyoshi@isc.chubu.ac.jp, motojima@kcn.jp

^{b)}Second author: y.k@m.tohoku.ac.jp

^{c)}Third author: satomoto@isc.chubu.ac.jp

Abstract. The novel proposal of the Muon Catalyzed Fusion (MCF) concept is brought to light employing recent results on its relevant cross sections. In 1993, Kino et al. proposed an innovative scheme of MCF, employing non-adiabatic calculations of muonic atom-nucleus collision in the energy range from 10^{-3} eV to 100 eV, whereby the fusion in flight along with the formation of muonic molecular resonances was revisited [1]. In 1994, Froelich independently calculated the cross section up to 2 keV, and found the behavior of like resonance [2]. In 1996, Kino et al. examined these resonances, and concluded that the resonances were not suitable for MCF [3]. As a result, the research has been continued to examine the possibility of non-resonant In-flight Muon Catalyzed Fusion (IFMCF) calculating the muonic atom-nucleus collision cross-section with an improved precision within the optical model for nuclear reactions. The resultant fusion cross section was 2000 barns at 1.4 keV [4] which should be good enough to be used as a fast neutron source [5]. A research program has been initiated to confirm these results theoretically as well as experimentally. For the sake of the theoretical analysis, a few-body computer code has been put forward to handle the nuclear reactions for nucleon transfer. In this paper, an innovative compact reactor concept is proposed, based on IFMCF. In this concept, muons are injected to a gas target of D₂ and T₂, which is pressurized aerodynamically by the Mach shock wave using a supersonic stream generated in a Laval nozzle [6], [7]. It generates the output power of 28 MW with 10^{19} cm⁻³s⁻¹ of fusions by supplying fresh muons of 10^{16} cm⁻³s⁻¹ providing 1000 times of catalyzed cycle of reactions. To maintain Q values > 1, assuming 30% efficiency for thermal to electric conversion, the energy supply for muon production can be as low as 8 GeV/muons. One of the possible applications of muon catalyzed fusion is transmutation of long-lived fission products (LLFPs).

1. INTRODUCTION

In the previous research of MCF [8]-[15], muonic fusion reactions were considered to take place mainly in dense matter, i.e., ice or liquid deuterium (D₂) and tritium (T₂). When muons are injected into the target, electron is replaced by negative muon (μ^-). Hence, muonic atom are produced, in which Bohr radius is reduced by a significant factor 207 compared to an ordinary atom. The evolution proceeds in following stages $d\mu$ or $t\mu$ formation (10^{-11} sec) \rightarrow muon transfer ($<10^{-8}$ sec) \rightarrow $dt\mu$ molecule formation ($<10^{-8}$ sec) [16]-[19] \rightarrow intramolecular nuclear fusion (10^{-12} sec) [20], [21] \rightarrow release muon with energy 10 keV. The process continues during the life time of muon (2.2×10^{-6} sec). The period of one cycle is approximately 2×10^{-8} sec. It was reported that this catalyzed cycle could be up to 150 times [22]. This scenario is termed Muon Catalyzed Fusion (MCF) and is illustrated in Fig. 1a.

In this context, the target has to be cold and highly dense, i.e. ice or liquid hydrogen form is required to attain fusion reactions. It should be pointed out that the target is heated by alpha particles resulting from fusion reactions. It expands and finally evaporates. Hence, the cold fusion cannot continue longer than 2 μ s at the generation rate of 10^{19}

$\text{cm}^{-3}\text{s}^{-1}$ of alpha particles. If a cold pellet of 1 cm^3 is injected during one microsecond, the speed of the injection must reach a very high value of 1000 m/s equal to the acoustic rate. Friction forces also heat the target making it difficult to maintain hydrogen isotopes in the form of ice or liquid. Vortexes in the liquid flow also produce heat by making micro bubbles. Therefore, it is generally asserted that the prospect of cold MCF remains not realistic [23]. If the cold solid or liquid target could be replaced by gas, the bottle neck problem of the MCF cycle called sticking can be resolved as illustrated in Fig. 1b. This is the new concept of In-Flight Muon Catalyzed Fusion (IFMCF) [24]. The number of muon catalyzed cycle increases significantly to the necessary level.

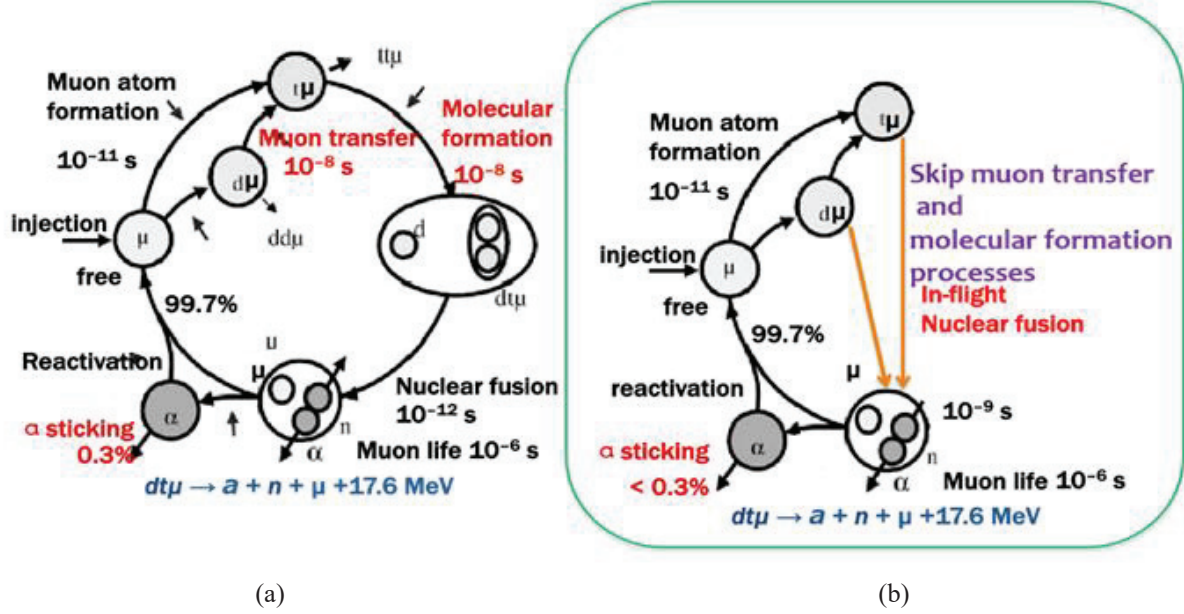


FIGURE 1. Comparisons of cold MCF and In-Flight MCF. (a) Conventional MCF cycle. The evolution proceeds in following stages $\text{d}\mu$ formation (10^{-11} sec) \rightarrow muon transfer ($<10^{-8} \text{ sec}$) \rightarrow $\text{dt}\mu$ molecule formation ($<10^{-8} \text{ sec}$) \rightarrow nuclear fusion \rightarrow release muon with energy 10 keV. The maximum number of muon cycling is about 100 during in the life time of a muon in conventional cold MCF. (b) In-Flight MCF cycle. The number of muon cycling increases dramatically to 1000 by the skipping muon transfer and molecular formation processes.

2. IN-FLIGHT MUON CATALYZED FUSION (IFMCF)

2.1. General Concept

In 1993, Kino et al. developed the non-adiabatic approach to calculate the fusion cross section over a wide collision energy range from 10^{-3} eV to 100 eV , and examined muon catalyzed fusion (MCF) in dissipative systems [1], [24]. In 1994, Froelich extended the range up to 2 keV , and found a resonance-like behavior in the cross section [2]. In 1996, Kino et al. continued to calculate the muon atom-nucleus collision cross section employing the optical model of nuclear reaction [25]. The height of the Coulomb barrier decreases by the factor of 207 and the quantum mechanical tunneling effect due to the non-adiabatic muonic motion as shown in Fig. 2. Indeed, the fusion cross section dramatically increases up to 2000 times within the range up to 1.4 keV . It is several hundred times larger than that of $\text{d}^+\text{-t}^+$ fusion in the bare nuclei without a muon.

$^5\text{He}\mu$ atom is formed momentarily as a result of overcome of the Coulomb barrier. It is highlighted in Fig. 3 [25]. The reason why the recycled muon has a mono-energy of 10 keV is explained that muons at the ground state of $^5\text{He}\mu$ are released at the end of the fusion reaction. The energy of the ground state of ^5He is -10 keV and the released muon obtains 10 keV so that the new idea is to use a thermal motion as a driver in the context of IFMCF.

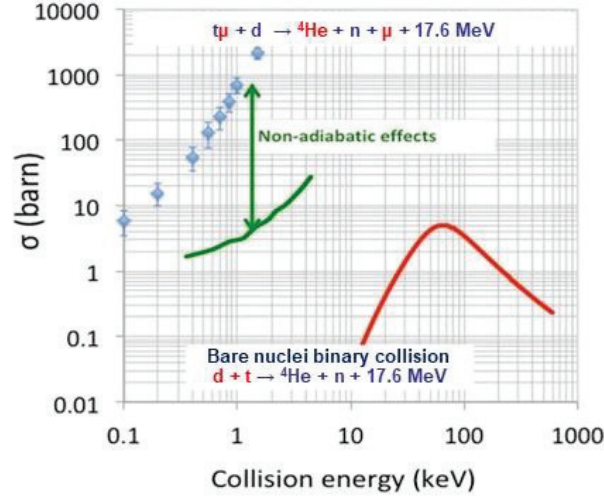


FIGURE 2. Enhancement of fusion cross section. Blue points show the cross section of binary nuclear reaction between the muon atom $t\mu$ and d . If we omit the closed channel, i.e. in adiabatic calculation, the cross section decreases by orders of magnitude as shown in green line. The energy of collisions is as one order low as thermonuclear fusions in red line.

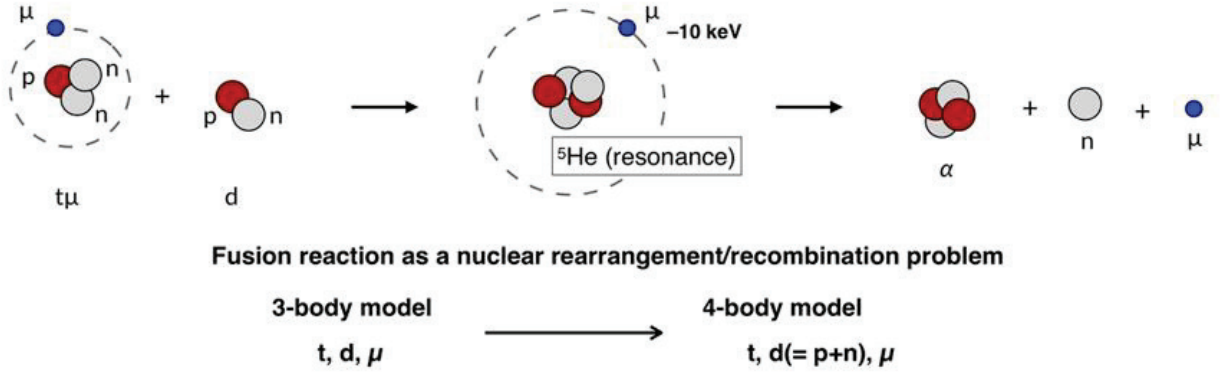


FIGURE 3. Schematic view of nuclear recombination during IFMCF reaction. The recycled muon has a mono-energy of 10 keV. The energy of the ground state of ${}^5\text{He}$ is -10 keV, therefore, the released muon obtains 10 keV.

2.2. Discussion on Kinetic Energy Transfer from muon to muon atom

Because the relative kinetic energy of 1-2 keV is necessary to facilitate IFMCF fusion reactions, it is necessary to develop a method to reach this energy level.

Slow muons stop in the range of a few mm in the high density gas target of 10^{21} cm^{-3} which corresponds to minimum 30 atm at room temp. Once deuterium and tritium atoms catch a muon, the muon falls in the energy bands from the outermost shell to the ground state as illustrated in Fig. 4. They are neither subjected to the bremsstrahlung loss like as electrons, nor experiencing inelastic collisions as ions. Therefore, muon atoms have a probability to obtain kinetic energy of 1-2 keV in the reduced mass system. The detailed analysis has been carried out to invoke wave functions in order to solve exactly a four-body problem.

The target gas is heated by fusion generated alpha particles of 3.5 MeV. They lose some energy due to non-elastic collisions such as excitation and ionization, and gain energy due to elastic collisions. Alpha particles produce low temperature plasma of 10-100 eV, of which energy decays in 100 ns. At the generation rate of $10^{19} \text{ cm}^{-3}\text{s}^{-1}$ of alpha particles, plasmas with densities of 10^{13} cm^{-3} are steadily formed. Some ions are excited up to 2 keV due to elastic collisions with alpha particles [26]-[30].

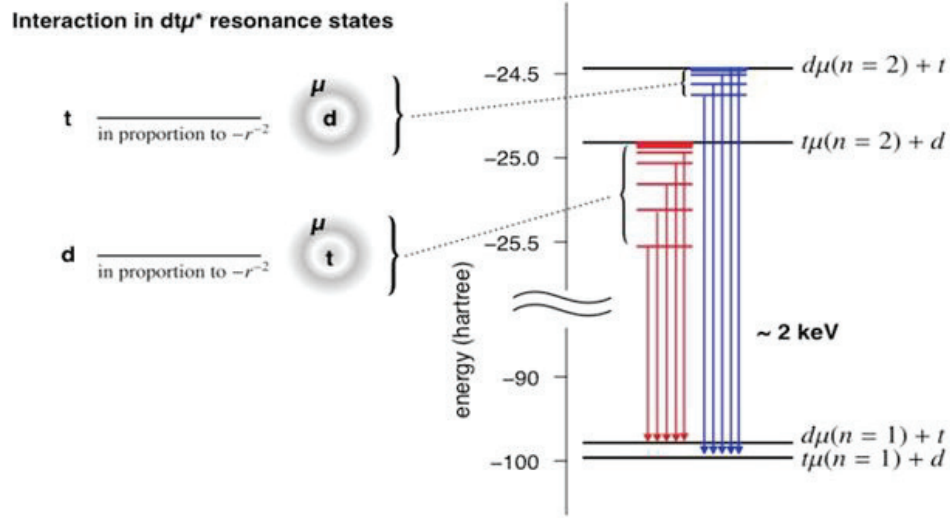


FIGURE 4. Particle emission decay in d+t muonic atoms. At the molecular stage muon located at the ground state of ${}^5\text{He}$ is released at the end of fusion process. The energy of the ground state of ${}^5\text{He}$ is -10 keV. Therefore, the released muon obtains 10 keV.

2.3. Lawson Criterion estimated for IFMCF

As is well known that, great efforts have been made to increase the energy confinement time to satisfy the Lawson Criterion of a fusion reactor especially in magnetic fusion, and in inertial fusion, to increase the product ρR (ρ : density and R : radius of reaction). Therefore, the question is which parameters would define the Lawson Criterion for IFMCF.

The major players of IFMCF are muons, muon atoms, and alpha particles, of which time from generation to annihilation is microsecond or less. All of them are spread by the classical diffusion. The reaction area of IFMCF is yielded by comparing ranges of the formation of muon atoms, fusion reactions with muon atoms resulting in neutral gases or plasmas, and alpha particle heating of neutral gas or plasma. At a fusion reaction rate of 10^{19} per second, these stopping ranges remain in a volume of 1 cm^3 .

The lifetime of muons is only $2.2 \mu\text{s}$, and during this short lifetime, muon catalyzed fusion reactions must unfold as often as possible. To this end, the collision time and reaction area should be reduced as much as possible. In the muon reaction of our interest, there are three important cross sections defining the process, namely, $\sigma_{\mu n}$: the collision between muon and neutral gas for muon atom formation, $\sigma_{\mu f}$: the collision between muon atoms and ions or neutral gas for fusion, $\sigma_{\alpha n}$: the energy loss cross section of the fusion alpha particle dependent on inelastic and elastic collisions with neutral gas atoms. The product of $n_i n_j \langle \sigma_{ij} v_{ij} \rangle$ defines the reaction rate per unit volume. Here, n_i , n_j , $\langle \sigma_{ij} v_{ij} \rangle$ are the number density, collision cross section and relative velocity, and suffix i and j denote kinds of particles. The mean free path λ_{ij} and mean collision time τ_{ij} of a projectile i and target j are given as $\lambda_{ij} = 1 / n_j \sigma_{ij}$ and $\tau_{ij} = 1 / (n_j \langle \sigma_{ij} v_{ij} \rangle)$.

These parameters determine the scale length in each step during a muon catalyzed cycle of IFMCF at a d-t fusion reaction rate of 10^{19} s^{-1} which would take 1000 cycles of catalyzed muon reaction. In this case, 10^{16} s^{-1} of fresh muons must be supplied to maintain the steady state operation. These mean free times and paths are calculated, using open computer codes, SLIM and TRIM [31].

In order to assess the issue of energy production, the fusion gain Q is estimated, which is the ratio of fusion power generated to heating power. Fig. 5 is a block diagram of an IFMCF reactor showing particle and energy flows. Since even under the most unfavorable assumption that the muon production consumes $2 \text{ GeV}/\mu\text{on}$, $Q \geq 1$ will be achieved. For this evaluation, we assumed that 50% of fresh muons are lost along with the transmission line and that only the $5 \times 10^{15} \text{ cm}^{-3} \text{ s}^{-1}$ of muons can reach the fusion zone. The analysis is based on the present performance of the highest energy particle accelerators.

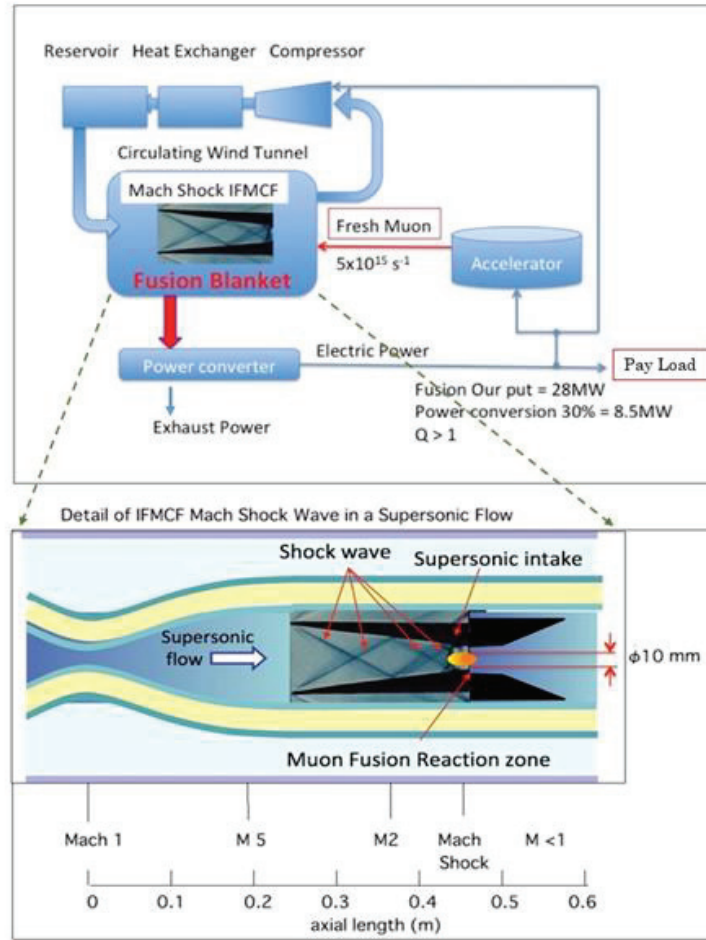


FIGURE 5. Block diagram of an IFMCF reactor. Assuming 50% of muons reaches to fusion zone, and a muon rounds 1000 cycles, it requires $2 \times 10^{16} \text{ cm}^{-3} \text{ s}^{-1}$ fresh muons to have accounts of $10^{19} \text{ fusion s}^{-1}$. The lower picture illustrates the application of a Laval nozzle. A pair of wedges generate oblique shock waves. Along with the flow, a Mach shock stays at the end of the wedge. The Schlieren picture shows an example of Mach shock formation for the Mach 4 scramjet inlet model by JAXA [33].

3. CONCEPT OF IFMCF REACTOR

The fusion area is created by the Mach shock wave generated along the supersonic flow in a Laval nozzle as illustrated in Fig. 5 [32], where a target gas is held, refueled and heat is removed. It stems from an oblique shock wave supported aerodynamically [33]. No magnetic field is needed to support fusion area. An IFMCF reactor could rely upon existing technologies. Although the fusion fluxes are much higher than that of magnetic fusion, such as DEMO, high density and high speed gas removes the alpha particle energy. Alpha particles with the energy of 3.5 MeV loses their energy in the stopping range of 5 mm. Temperature rise rate is estimated about $400 \text{ K}/\mu\text{sec}$, and is taking out in a micro sec.

Assuming a catalyzed reaction using muons for 1000 cycles, fusion reaction would take place at a rate of $10^{19} \text{ cm}^{-3} \text{ s}^{-1}$. This might provide an idea of a compact fusion reactor with a thermal output of 28 MW and an electrical output of 10 MW.

One of the possible applications of the concept of IFMCF reactor is a neutron source for the transmutation of long-lived fission products (LLFPs) from present-day nuclear power plants. According to our calculations by applying PHITS code [34]-[36], fast neutron fluxes of the order of $10^{19} \text{ m}^{-2} \text{ s}^{-1}$ can convert 10-100 kg of LLFPs to stable nuclei or short-lived radioactive isotopes with the half -life of 10 years. The LLFP blanket covers the reactor core and the

outside area is filled with the light water for absorption of neutrons and heat recovery. It is envisaged that the reactor can be exploited for many other purposes and not only for converting LLFPs into stable or short-lived nucleus without any generation of unnecessary nuclei.

4. SUMMARY

- The technical issues associated with the concept of In-Flight Muon Catalyzed Fusion (IMFCF) are addressed in this article.
- IMFCF does neither require either tight energy balance as required for magnetic fusion, or homogeneous implosion required for inertial fusion.
- Main supplying energy is the consumption for muons production. No other energy input is required.
- The energy output can exceed the input energy.
- Steady state and stable operation can be maintained in an open system where the energy input from the outside is minimal.
- IFMCF is a system that is well adapted to existing technology and can be realized in a relatively short time.
- The cost of electricity by IFMCF can reasonably be reduced as existing nuclear power plants.
- From the experimental point of view, cross sections of MCF should be measured by muon producing facilities in Japan.

ACKNOWLEDGMENTS

We would like to our heartfelt thanks to Professor Hironori Sakurai of RIKEN/Tokyo University for promoting the coupled research on MCF fusion and the transmutation of LLFP. We are deeply appreciating to Dr. Akihiro Matsubara, Prof. Hirohisa Takano, Dr. Aki Fujita, Prof. Takeshi Kanda, Prof. Takashi Mutoh, Prof. Yoshi Hiroka, Prof. Kimitaka Ito and Associate Prof. Yury Ivanov of Chubu University for their valuable scientific and technological suggestions.

The research started under the support of the Japanese government's program "Impulsing Paradigm Change through Disruptive Technologies Program" (ImPACT). This work is supporting by JSPS KAKENHI Grant Number JP 17K05592 for the theoretical research and 18H05461 for the experiments to proof of principle. The PHITS (Particle and Heavy Ion Transport code System) were used for simulation to the LLFP transmutations.

REFERENCES

1. Y. Kino and M. Kamimura, [Hyperfine Interact.](#) **82**, 45-52 (1993).
2. P. Froelich, A. Flores-Riveros, J. Wallenius, and K. Szalewicz, [Phys. Lett. A](#) **189**, 307-315 (1994).
3. Y. Kino and M. Kamimura, [Hyperfine Interact.](#) **101**, 191-196 (1996).
4. Y. Kino, T. Yamashita, T. Oka, and M. Sato, *Proc. of 2018 Fall Meeting Atomic Society of Japan*, Okayama, Japan, (2018), 2N02.
5. N. Yamamoto, M. Sato, H. Takano, and A. Iiyoshi, *Proc. of 2018 Fall Meeting Atomic Society of Japan*, Okayama, Japan, (2018), 2N01.
6. M. Sato, Y. Kino, Y. Tanahashi, N. Yamamoto, H. Takano, T. Mutoh, A. Fujita, A. Iiyoshi, and A. Matsubara, *Proc. of 2018 Fall Meeting Atomic Society of Japan*, Okayama, Japan, (2018), 2N03.
7. Y. Tanahashi, *Proc. of 2018 Fall Meeting Atomic Society of Japan*, Okayama, Japan, (2018), 2N05.
8. K. Nagamine, *Introductory Muon Science* (Cambridge University Press, Cambridge, 2003).
9. C. D. Anderson and S. H. Neddermeter, [Phys. Rev.](#) **50**, 263-271 (1936).
10. J. C. Street and E. C. Stevenson, [Phys. Rev.](#) **52**, 1003 (1937).
11. F. C. Frank, [Nature](#) **160**, 525-527 (1947).
12. J. D. Jackson, [Phys. Rev.](#) **106**, 330-339 (1957).
13. E. A. Vesman, *Sov. Phys. JETP Lett.* **5**, 91-93 (1967).
14. C. S. Wu and L. Wilets, [Ann. Rev. Nucl. Sci.](#) **19**, 527-606 (1969).

15. S. S. Gerstein and L. P. Ponomarev, *Phys. Lett. B* **72**, 80-82 (1977).
16. S. Hara and T. Ishihara, *Phys. Rev. A* **40**, 4232-4236 (1989).
17. C. Y. Hu and A. K. Bhatia, *Phys. Rev. A* **43**, 1229-1232 (1991).
18. P. Froelich and A. Flores-Riveros, *Phys. Rev. Lett.* **70**, 1595-1598 (1993).
19. P. Froelich and J. Wallenius, *Phys. Rev. Lett.* **75**, 2108-2111 (1995).
20. L. I. Ponomarev, *Contemp. Phys.* **31**, 219-245 (1990).
21. S. Eliezer and Z. Henis, *Fusion Technol.* **26**, 46-73 (1994).
22. S. E. Jones, A. N. Anderson, A. J. Caffrey, C. DeW. Van Siclen, K. D. Watts, J. N. Bradbury, J. S. Cohen, P. A. M. Gram, M. Leon, H. R. Maltrud, and M. A. Paciotti, *Phys. Rev. Lett.* **56**, 588-591 (1986).
23. K. Nagamine, RIKEN Accel. Prog. Rep. **50**, 39-42 (2017).
24. E. Hiyama, Y. Kino, and M. Kamimura, *Prog. Part. Nucl. Phys.* **51**, 223-307 (2003).
25. T. Yamashita, M. Umair, and Y. Kino, *J. Phys. B* **50**, 205002 (2017).
26. N. Kawamura, K. Nagamine, T. Matsuzaki, K. Ishida, S. N. Nakamura, Y. Matsuda, M. Tanase, M. Kato, H. Sugai, K. Kudo, N. Takeda, and G. H. Eaton, *Phys. Rev. Lett.* **90**, 043401 (2003).
27. M. Papa, T. Maruyama, and A. Bonasera, *Phys. Rev. C* **64**, 024612 (2001).
28. M. Jandel, M. Danos, and J. Rafelski, *Phys. Rev. C* **37**, 403-406 (1988).
29. H. Takahashi, *Muon Cat. Fus.* **5/6**, 363 (1990/1991).
30. D. Harley, *Phys. Rev. A* **45**, 8981-8983 (1992).
31. SRIM and TRIM code, <http://www.srim.org/SRIM/SRIMLEGL.htm>
32. Y. Tanahashi, T. Ohara, and Y. Nakamura, *J. Spacecraft Rockets* **36**, 681-687 (1999).
33. T. Kanda, T. Komuro, G. Masuya, K. Kudo, and A. Murakami, *J. Propul. Power* **7**, 275-280 (1991).
34. K. Niita, T. Sato, H. Iwase, H. Nose, H. Nakashima, and L. Sihver, *Radiat. Meas.* **41**, 1080-1090 (2006).
35. H. Iwase, K. Niita, and T. Nakamura, *J. Nucl. Sci. Technol.* **39**, 1142-1151 (2002).
36. K. Shibata, O. Iwamoto, T. Nakagawa, N. Iwamoto, A. Ichihara, S. Kunieda, et al., *J. Nucl. Sci. Technol.* **48**, 1-30 (2011).